Sediment delivery modeling in practice: comparing the effects of watershed characteristics and data resolution across hydroclimatic regions

Perrine Hamel[a,*], Kim Falinski[b], Rich Sharp[a], Daniel A. Auerbach[c], María Sánchez-Canales[d], James Dennedy-Frank[a,e]

[*]Corresponding author: perrine.hamel@stanford.edu

[a] Natural Capital Project, Woods Institute for the Environment, 371 Serra Mall, Stanford, CA 94305–502, USA. perrine.hamel@stanford.edu, richsharp@stanford.edu

[b] The Nature Conservancy, Hawaii Marine Program, 923 Nuuanu Avenue, Honolulu, HI 96817, USA. kim.falinski@tnc.org

[c] Office of Wetlands, Oceans and Watersheds, US-EPA, 1301 Constitution Avenue, Washington DC, USA. auerbach.daniel@epa.gov

[d] Universidad Politécnica de Madrid, Escuela Técnica Superior de Ingenieros de Minas y Energía, C/Ríos Rosas 21, 28003 Madrid, Spain. mscanales@dmami.upm.es

[e] Stanford University, Department of Earth System Science, Yang & Yamazaki (Y2E2) Building, 473 Via Ortega, Stanford, CA 94305-4216, USA. pjdf@stanford.edu

Abstract

Geospatial models are commonly used to quantify sediment contributions at the watershed scale. However, the sensitivity of these models to variation in hydrological and geomorphological features, in particular to land use and topography data, remains uncertain. Here, we assessed the performance of one such model, the InVEST sediment delivery model, for six sites comprising a total of 28 watersheds varying in area (6-13,500 km^2), climate (tropical, subtropical, mediterranean), topography, and land use/land cover. For each site, we compared uncalibrated and calibrated model predictions with observations and alternative models. We then performed correlation analyses between model outputs and watershed characteristics, followed by sensitivity analyses on the digital elevation model (DEM) resolution. Model performance varied across sites (overall $r^2 = 0.47$), but estimates of the magnitude of specific sediment export were as or more accurate than global models. We found significant correlations between metrics of sediment delivery and watershed characteristics, including erosivity, suggesting that empirical relationships may ultimately be developed for ungauged watersheds. Model sensitivity to DEM resolution varied across and within sites, but did not correlate with other observed watershed variables. These results were corroborated by sensitivity analyses performed on synthetic watersheds ranging in mean slope and DEM resolution. Our study provides modelers using InVEST or similar geospatial sediment models with practical insights into model behavior and structural uncertainty: first, comparison of model predictions across regions is possible when environmental conditions differ significantly; second, local knowledge on the sediment budget is needed for calibration; and third, model outputs often show significant sensitivity to DEM resolution.

1 Introduction

Sediment transport models seek to represent the sources and volumes of sediment leaving a basin. Predictions from such models help inform landscape management decisions at various spatial scales. For example, estimates of sediment export have supported global ecosystem service assessments, highlighting the value of native vegetation and exposing vulnerabilities under scenarios of land use or climate change (e.g. Water blueprint by McDonald and Shemie, 2014). At smaller scales, sediment models can support the design of watershed management plans that balance agricultural development, domestic water demand, and biodiversity conservation (e.g. Goldman-Benner et al., 2012).

A number of practical applications necessitate spatially-explicit information on sediment yields. Given their relative simplicity and the growing availability of environmental data, geographic information system (GIS)-based models are increasingly used: a major application is to identify zones of high or low sediment yield, thereby supporting decisions to prioritize sites for restoration or implementation of best practices. Alternatively, these tools may be used for predictions of sediment yield under particular scenarios of climate or land cover change (e.g. Hamel et al., 2015). GIS-based models can also contribute to basic research toward refining sediment budgets by distinguishing the contributions from sources such as sheet, gully, and bank erosion (de Vente et al., 2013).

An important class of spatially distributed models combine an estimate of soil erosion with a transport model, which represents the amount of sediment actually reaching the watershed outlet (e.g. GWLF, SWAT, SEDEM, AGNPS models, reviewed by de Vente et al. 2013). Estimates of soil erosion can be derived from empirical models such as the Universal soil loss equation (USLE) or its variants RUSLE/MUSLE (see review by Merritt et al., 2003), or from the direct use of empirical export coefficients (e.g. White et al., 2015). Soil loss estimates are then combined with information on sediment transport, or *connectivity*, which is defined as "the integrated transfer of sediment across all possible sources to all potential sinks in a system over the continuum of detachment, transport and deposition" (Bracken et al., 2015).

In recent years, measures of sediment connectivity have been derived from geographic datasets that describe environmental features with basic assumptions about how sediment is transported across the landscape to the stream. These datasets typically include topography, intensity and frequency of precipitation events, and land use/land cover (LULC) (Bracken et al., 2013). For example, Borselli et al. (2008) implemented and tested a theory of landscape hydrologic connectivity via an index that is computed from geospatial raster data, specifically a digital elevation model (DEM) and a LULC map used to derive slope, flow accumulation, and landscape “roughness”. The connectivity index can subsequently be used to calculate sediment delivery ratios (SDR), representing the proportion of eroded soil on a pixel that eventually reaches the stream.

The algorithm from Borselli et al. described above was recently adapted and integrated into the InVEST software, a suite of tools that aims to assess ecosystem services (Sharp et al., 2016). The model showed good performance in a range of environments, explaining a large proportion of the variance in sediment yields for nested watersheds in United States (Hamel et al. 2015). Other studies conducted with the original algorithm developed by Borselli also found that the model was able to predict variability in sediment yields in Italy, South-East Australia and Hawai’i (Cavalli et al., 2013; Falinski, 2016; Leombruni et al., 2009; Vigiak et al., 2012).

Despite these encouraging results and the utility of GIS-based models for landscape planning, the level of confidence associated with these models remains unclear. In particular, uncalibrated results difficult to ascertain, and model comparisons across regions are rare, making it difficult to distinguish model noise from actual differences in sediment exports (Chaplin-Kramer et al., 2016). For example, the optimal value of the main calibration parameter, k_b (see Section 2.1), was 2 in Australian catchments (Vigiak et al., 2012) and 1.8 in North Carolina (Hamel et al., 2015). Such difference is expected given the empirical nature of the model but better guidance and regional insights would improve uncertainty assessment and modeling practice.

Among the factors influencing model predictions, DEM resolution plays a particular important role: in fact, both pixel-scale soil loss (computed via a grid-based implementation of the USLE), and the SDR factor are functions of pixel size. Recent studies have aimed to quantify the effect of DEM resolution on hydrologic predictions: for example, Zhu et al. (2014) showed that for six watersheds in China, the accuracy of the slope-length factor decreased with increasing DEM resolution and terrain complexity. Mondal et al. (2016) show that increasing DEM resolution can decrease soil loss estimates by >12% in their catchment in India, and these trends were similar to those found by Lin et al. (2013) and Wu et al. (2005). Although this body of literature confirms the importance of the DEM effect, limited practical guidance is currently available to model users. With regards to sediment connectivity, and therefore the SDR factor, the algorithm used in the calculation of sediment connectivity showed limited sensitivity to DEM resolution in a subset of Australian watersheds (Vigiak et al. 2012), although these results cannot be extrapolated to other geographies.

In this paper, we propose to advance the understanding of the above two issues: the effect of environmental factors on one hand, and of DEM resolution on the other hand, on model performance and usefulness, with implications for both researchers and practitioners. Through six recent applications of the InVEST sediment delivery model, we assess the effect of topography and land cover on the sediment export computed by the model and perform sensitivity analyses on the effects of DEM resolution, for the six watersheds and a range of synthetic watersheds. These analyses provide important insights into the structural uncertainty of the InVEST model. Results also have implications for a range of GIS-based sediment models using a similar modeling philosophy (the coupling of a soil loss module with a transport module). Recognizing the demand for practical guidance from the environmental modeling community, we propose in our conclusion a set of practical recommendations that are relevant to practitioners using such models.

2 Methods

2.1 Study sites

The six sites used in this study are located in the contiguous U.S., Hawai'i, Puerto Rico, Kenya, and Spain, thus representing Mediterranean, tropical and subtropical climates (Figure 1; Table 1 summarizes key watershed characteristics). Relief varies greatly, with median slopes ranging from 4 to 72% (see Table 1 for ranges), and are dominated by forest and crops (Tana). Each site was used in previous work by the authors such that model inputs, observations and alternative model predictions were readily available (see Supplementary Material). In total, they constitute a dataset of 28 subwatersheds, with between two and eight subwatersheds in each site. Note that data sources differ between sites: for example, erosivity was obtained directly from governmental agencies' datasets for the U.S. sites, while it was derived from precipitation data and empirical equations for other sites. Similarly, C and P factors (see below for a description of these parameters) were obtained from different regional sources; therefore, they have different values in each site.

2.2 Model overview

The InVEST sediment delivery model implements a soil loss algorithm linked to the sediment connectivity algorithm proposed by Borselli et al. (2008). Soil loss is computed with the revised universal soil loss equation (RUSLE) for each pixel (Renard et al., 1997). The equation multiplies five factors corresponding to the erosivity (R; related to the energy from precipitation that is available to move particles), erodibility (K; reflecting soil physical properties that define susceptibility to particle removal), slope-length (LS; related to the topographic context for particle movement), and two empirical factors related to the land use-land cover: the cover factor, C, and the practice factor, P. The LS factor is computed with D-infinity routing following the expression developed by Desmet and Govers (1996) and implemented in the PyGeoprocessing library (Sharp et al. 2016).

Soil loss is then multiplied by a sediment delivery ratio (SDR) factor, computed for each pixel according to the sediment connectivity algorithm (Borselli et al., 2008; Cavalli et al., 2013). The product of soil loss and the SDR factor is the sediment export from each pixel (see example map in Figure S1). The SDR factor is a function of the index of connectivity, which is itself a function of the upslope contributing area and downslope flow path of a pixel (cf. Figure 1a in Hamel et al. 2015). Specifically, SDR and IC are related to the C-factor and slope according to the following equations (computed on each pixel):

$$IC = log_{10}\left(\frac{D_{up}}{D_{dn}}\right), \quad (1)$$

where D_{up} is the upslope component defined as:

$$D_{up} = \bar{C}\bar{S}\sqrt{A}, \quad (2)$$

with $\bar{C}$ is the average C factor of the upslope contributing area, $\bar{S}$ is the average slope gradient of the upslope contributing area (m/m) and A is the upslope contributing area (m^2). The upslope contributing area is delineated from the D-infinity flow algorithm (Tarboton, 1997).

The downslope component D_{dn} is given by:

$$D_{dn} = \sum_i \frac{d_i}{C_i S_i}, \quad (3)$$

where d_i (m) is the distance along the steepest downslope direction from the i^{th} pixel to the first downslope stream pixel; C_i and S_i are the C factor and the slope gradient of the i^{th} pixel, respectively (Figure 1a in Hamel et al., 2015). The hydrographic network (stream pixels) is extracted from the DEM using a threshold flow accumulation parameter, TFA, corresponding to the number of pixels (or, equivalently, the area) necessary to initiate channel flow.

The sediment delivery ratio for a given pixel i is derived from the connectivity index IC using a sigmoid function:

$$SDR = \frac{SDR_{Max}}{1+\exp\left(\frac{IC_0 - IC}{k_b}\right)}, \quad (4)$$

where SDR_{max} , k_b, and IC_0 are model parameters. Additional details and a sensitivity analysis for the Cape Fear watershed can be found in previous work (Falinski, 2016; Hamel et al., 2015). Model calibration is usually done by changing the k_b value following the approach explained by Hamel et al. (2015), aiming to minimize the model bias on sediment export. Details for each site are provided in Supplementary Material. IC_0 is also used as a calibration parameter, which is the case for the Hawai‘i site in this study (cf. Supplementary Material, Section 2).

2.3 Comparison of sediment export

For each subwatershed, we first computed the specific sediment export, defined as sediment export normalized by watershed area, obtained from the uncalibrated InVEST model. We compared these estimates to specific sediment exports obtained from at least one of the following methods (depending on data availability): InVEST calibrated model, direct observations (obtained either from bathymetric survey or sediment concentration time series), alternative deterministic model (SWAT), and two statistical models (BQART, Syvitski and Milliman, 2007; and FSM, Verstraeten et al., 2003). The two statistical models permitted a comparison of InVEST to alternative approaches with modest data and time requirements, while the comparison to SWAT outputs served as reference to approaches with greater complexity.

The Supplementary Material provides additional details on processing of observed data or alternative sources for the “best estimate” for sediment export at each subwatershed, as well as execution of individual models at each site (InVEST and alternative models). We selected BQART and FSM based on a review by de Vente et al. (2013) for regional sediment yield models, focusing on models that had low data and computational requirements (lumped models). BQART uses data on runoff (Q), area (A), relief (R), temperature (T), lithology, glaciology and human influence (B) to predict sediment yield. It was verified on 488 catchments worldwide, accounting for 95% of the variance in sediment loads. Runoff values were taken from previous studies when available (Cape Fear, from Hamel and Guswa, 2014, and Llobregat, from Terrado et al. 2013), or from Figure 1 in the original BQART paper by Syvitski et al. 2007. Temperature data were taken from Figure 1 in Syvitski et al. 2007. FSM uses five factors characterizing vegetation, topography, presence of gullies, lithology, and shape to predict sediment yield. It was tested on 96 catchments and explained between 67 and 87% of the variance (de Vente et al. 2013). For some of the catchments studied in this work, the regression equation of FSM yielded negative values and the predictions were therefore discarded. Section 7 of the Supplementary Material summarizes sediment export estimates from each model.

2.4 Correlation between sediment delivery metrics and watershed characteristics

A major objective of this paper is to understand how watershed characteristics influence the sediment export and sediment delivery ratio factor (SDR, the proportion of exported sediment relative to eroded soil for a given pixel). With this aim, we analyzed the correlation between SDR and a range of watershed variables related to topography, climate, soils, and vegetation, as summarized in Table 2.

2.5 Sensitivity of sediment delivery metrics to DEM resolution

2.5.1 Empirical analyses

For each site, we created a 30-m, 90-m, and 180-m DEM based on the finest available resolution for the site (10 or 15 m). Recent literature suggests that the choice of the resampling method does not influence results significantly in studies of DEM resolution (Wu et al., 2008). Here, we used the bilinear interpolation to resample DEM to coarser resolutions. We re-ran each calibrated model with these DEMs to compare the soil loss (USLE) and sediment export for each resolution. The threshold flow accumulation parameter, describing the number of upstream pixels contributing flow to the point of stream channel initiation, was adjusted to match the pixel size from resampled rasters using the following equation:

$$TFA_1 = TFA_0 \left(\frac{r_0}{r_1}\right)^2, \quad (5)$$

where TFA and r represent, respectively, the threshold flow accumulation and the resolution for the initial (“0”) and new (“1”) DEMs.

2.5.2 Numerical analyses

To assess the effect of DEM resolution on model outputs, we conducted a sensitivity analysis of InVEST output variables with a synthetic watershed ‘template’ (Figure 2). Our goal here was not to investigate multiple topographic features but to gain insights into how InVEST variables varied with DEM resolution for a simplified topography. The watersheds templates are 10 km-side squares draining to the center of one side, and created in Python. The function used to construct the elevation (Figure 2, left) assigns each pixel a height value as a function of the horizontal distance to the watershed drain, multiplied by a constant factor to adjust mean slope, and offset by a small random value to generate a non-trivial stream network (Figure 2, left). Formally, pixel’s height in the synthetic landscape is:

$$height_p(d) = d * s + rand(p) \quad (6)$$

where d is the distance of pixel p to the watershed drain, s is the mean slope of the watershed, and *rand(p)* generates a random number between -1 and 1. Five synthetic watersheds were built from this template, with a mean slope of 2, 5, 10, 15, and 5 m/m, respectively.

From each template, we created 40 watersheds with distinct DEM resolutions, starting from 5 m and increasing to the coarsest resolution of 200 m by increments of 5 m, and computed sediment variables with the InVEST model. Erosivity and erodibility are homogeneous across the area (equal to 1 unit). LULC is also assumed homogeneous for four of the watersheds, with C and P factors set to 0.1 and 1, respectively. For the fifth watershed template, with a 5 m/m-mean slope DEM, we used a two-class LULC raster with the C factor equal to 0.1 in the upper part, and 0.5 in the lower part (Figure 2, right).

3 Results

3.1 Comparison of sediment exports

Specific sediment exports, which by definition discard the effect of watershed area, varied widely across sites. Values ranged from 0.98 ton/km^2/yr in Cape Fear, to more than 3100 ton/km^2/yr in Puerto Rico (see Supplementary Material for discussion of these high yields).

The calibrated InVEST model predicted the relative magnitude of specific sediment yields (Figure 3) with relatively good accuracy (r^2 of 0.47). Uncalibrated model performance was lower (r^2 of 0.39), although relative differences between sites were generally correctly predicted (crossed square in Figure 3). In general, relative errors were lower for the uncalibrated model than the one obtained with the BQART and FSM models (for comparison, r^2 for both models is <0.03).

3.2 Correlation between sediment delivery metrics and watershed characteristics

We found a significant relationship ($p<0.05$) between the SDR median value, watershed area, erosivity, erodibility, and the percentage of urban areas and other LULC in the landscape (Table 3). Contrary to our expectations, we found no relationship between the SDR median value and any of the slope metrics, although there was a weak ($r=-0.41$) correlation between the 10th percentile of SDR values and the median slope. To help interpret these results, we also examined the correlation coefficients with the IC median value, a variable that is not affected by calibration: a significant relationship was also found with the percentage of LULC areas, but the correlation with the watershed area and erosivity and erodibility weakened. The 10th and 90th percentiles for each metric yielded generally similar results.

The large variability in topography and LULC between sites may confound some of these relationships. Therefore, we looked at correlations between variables within a site, Cape Fear, which was the one with the most subwatersheds for correlation analyses. We found the same trends as those presented in Table 3 (i.e. levels of significance and order of magnitude of the correlation coefficients were generally similar).

3.3 Sensitivity of sediment delivery metrics to DEM resolution

3.3.1 Empirical validation

The DEM resolution did not have a consistent effect on sediment export between sites, and the effect of increasing resolution differed both between sites and within sites (Figure 4). Relative to the highest resolution original baseline (either 10 or 15 m, depending on the site), the change in sediment export approximately ranged from -70% to 20%.

For some sites (e.g. Cape Fear), sediment export decreased with increasing resolution, while for others (e.g. Llobregat 2), the trend was positive. For yet other sites (e.g. Upatoi), sediment export did not show a monotonous trend.

Given the inconsistent trends, we explored the effect of DEM resolution on the SDR and RUSLE rasters separately: as explained in the next section, because sediment export from a pixel is the product of these two variables, its sensitivity to DEM resolution is affected by the sensitivity of each of the two variables. Similar to the data presented in Figure 4, we computed the change in USLE and SDR (compared to the baseline) for all sites. For some watersheds, the effect of DEM resolution on both USLE and SDR was cumulative, whereas it had opposite directions for other sites. Across the six sites, this compensatory effect, i.e. when the effect of DEM resolution has a different direction for USLE and SDR, seems to be common since most of the watersheds exhibited non-uniform trends (similar to Upatoi or Tana in Figure 4).

3.3.2 Numerical analyses

For all the synthetic watersheds, we saw an increase in total sediment export as DEM resolution coarsened. The relative difference between the 5-m and the 200-m resolution ranged from 5 to 10% for the five synthetic watersheds.

Figure 5 illustrates this trend for the 5 m/m-slope watershed, with homogeneous LULC, showing that sediment export increased by 10% for the 200-m resolution. This increase seems to be driven by the increase in total soil loss (+20%) and the median value of the SDR factor across the landscape, which both increase. However, given that the sediment export on a pixel is the product of soil loss and the SDR factor, we expected a sharper relative increase in sediment export (>10%). It appears that the trend in the median SDR value is not representative of SDR values across the landscape. For high values of SDR, e.g. 90th percentile, we observed a decreasing trend (orange line in Figure 5). This explains the trends in Figure 4: for some topographies, there exists a compensatory effect between soil loss and sediment delivery – the former increases while the latter decreases with coarser resolutions – *for pixels with the highest SDR values.* These pixels, which are more connected to the stream, contribute the most to the total sediment export and their response to coarsening resolution has a major influence on this output.

4 Discussion

Magnitude of sediment export predictions

Our analyses provide insight into the performance of the InVEST model when used across regions. Figure 3 shows that the InVEST model performance in our study watersheds was superior to global empirical tools for both the uncalibrated and calibrated models. This is partly due to the use of the RUSLE, which accounts for major environmental differences between sites (i.e. climate, through the erosivity, soils, through the erodibility). However, the transport component of the InVEST model (the SDR factor) also explains 39% of the variance in calibrated sediment exports (correlation between the 90^{th} percentile of the SDR values and calibrated exports), suggesting that both components of the model contribute to the reasonable prediction of sediment exports.

The difference between uncalibrated and calibrated model predictions was important, reducing bias by as much as 200% for some sites. This difference calls for caution in the interpretation of uncalibrated absolute values of sediment yields and should prompt users to think about the model's structural and parameter uncertainty. Parameter uncertainty is inevitable and can be quantified with simple sensitivity analyses (e.g. Hamel et al., 2015). There are also numerous reasons proposed for the differences between observed and modeled results, related to simplification of the processes represented by InVEST: for example, instream deposition and additional sediment sources such as bank erosion, gullies, landslides, or legacy sediments (e.g. in Hawai'i, see Supplementary Material) are not captured by the model. Recent work by Broeckx et al. (2016) suggests that in landscapes dominated by landslides, the SDR index or other distance-to-stream metrics were not a strong predictor of sediment yields. In such case, the major part of the sediment budget will not be adequately represented by the sheetwash erosion predicted by the model.

Of note, the calibration process used in this study assumes that sediment observations represent sheetwash erosion only, since this is the only process represented by the model. (One exception is for Cape Fear, where instream sedimentation was taken into account to correct sediment exports.) This simplification means that the spatially-explicit soil loss derived from the RUSLE is used as a proxy for other sediment sources. In doing so, the calibration process also compensates for the difference between sheetwash erosion and the total sediment production on a given pixel. While this is not the primary application of the model, it can prove useful in some applications where one can assume that the variations in RUSLE-based soil losses is representative (e.g. gully erosion may be driven by similar factors as sheetwash erosion).

Factors influencing the SDR and the sensitivity to DEM

Our correlation analyses indicated that the median SDR was sensitive to watershed area. This was unexpected given that the model structure is agnostic to this parameter: only the ratio of upslope area to downslope flow path (until the stream) is used. We suggest that this correlation can be explained by the calibration process. In fact, the correlation between sediment export and watershed area has been recognized for a long time (see de Vente et al., 2007), and our dataset of observed data exhibits this relationship. Therefore, the process of model calibration results in the predicted sediment export values to exhibit this relationship. This hypothesis is corroborated by the fact that the IC values, which are not affected by the calibration process, did not show any correlation with the area. Of note, the absence of correlation between IC values and watershed area are due to the implementation of the sediment delivery algorithm, which uses stream pixels as the “target” for downstream flow paths. An alternative algorithm uses the watershed outlet as the target, i.e. flow paths continued along the streams until the outlet. This formulation, examined by Cavalli et al. (2013) makes IC values sensitive to watershed areas but is not preferred for sediment delivery given the different processes involved in channel transport.

The SDR values showed a strong correlation with erosivity, which can be explained by the role of erosivity in watershed connectivity: in fact, high values of rainfall intensity are associated with higher delivery of sediment. Empirical evidence of such relationship was recently found in the Latrobe River catchment, Australia, where Vigiak et al. (2016) showed that periods of drought were associated with lower hillslope connectivity. Of note, we also examined the relationship between the SDR metrics and watershed runoff but found weak (and negative) correlation, suggesting that erosivity is a better proxy for watershed-scale connectivity in our study. We only found weak (and negative) correlation with the slope metrics. We expected such relationships given the presence of slope in the SDR equation, although it is possible that the proxies used in this study (percentiles of raster values) present an oversimplified picture of these relationships.

The correlation between SDR metrics and erosivity could be used for the development of heuristic approaches to estimate SDR values, and thus calibration values. Based on the six sites, the linear relationship (r^2=0.38) between the calibration parameter and median erosivity is:

$$k_b = 1.56 + 0.0002 * median(K) \tag{7}$$

Of note, this relationship is given here as a starting point for future research and we recognize that our sample size is small and that a number of factors may confound this relationship in new sites. For example, the correlation with the LULC metrics indicates that the SDR factor might be affected by values of the C-factor for particular classes. In our study, the percentage of urban and other classes showed a high correlation, which reflects the relatively lower values of the urban areas selected in a number of sites: for example, in Cape Fear, C-factor is 0.1, whereas it is 0.25 for agriculture (corn), which means that an increase in urban areas at the detriment of agricultural areas has the general effect of reducing the average C-factor.

Importantly, the sensitivity analyses on synthetic watersheds allowed us to disentangle the relationship between sediment export and DEM resolution. We confirmed the presence of a compensatory effect between the USLE and SDR variables (at the pixel scale), which we also observed with empirical data. The trends could not be simply associated with watershed characteristics, which means that predicting the direction of change of sediment export with a change in DEM resolution, let alone the magnitude of this change, remains a challenge. Of note, the LS factor (and thus soil loss values) in our synthetic watersheds increased with increasing resolution whereas it decreases in the watersheds studied by Mondal et al. (2016). This is due to the concavity of the hillslopes (U-shape in our study). Further work is needed to better determine the relationship between topographic indices and the USLE and the SDR values (see Reaney et al. (2014) for similar work for overland flow connectivity).

5 Conclusion and practical implications

Geospatial models are increasingly used for both research and practical management questions. The analyses presented here provide some useful practical insights into the behavior of one such model, the InVEST sediment delivery model. In particular, our comparison with alternative global models suggests that the use of the USLE captures some useful environmental characteristics, meaning that the model performance for regional comparison was fair even without calibration. In addition, the sensitivity analyses on synthetic watersheds demonstrated the possibility that the SDR factor and the USLE-based soil loss varied in opposite directions as DEM resolution increased, which means that their product, the sediment export, may only be mildly affected by changes in resolution. However, empirical data suggest that this is not the case for all topography, and predicting these relationships remain challenging for real, complex terrains (Baartman et al., 2013).

A number of practical questions have been raised in this study related to the model performance for ungauged and gauged watersheds and how watershed topography and DEM resolution affect model outputs. Although further research is needed to answer these questions with more confidence, we propose here a list of practical implications of this work. First, we suggest that comparison of InVEST predictions across regions is possible but should be accompanied by relatively simple verifications: DEM resolution should be comparable, and estimates of sediment yields should be verified against available data. As noted earlier, the model was able to capture sediment export variability when important environmental differences were seen between sites (e.g. erosivity and erodibility); however, the noise in Figure 3 prevents a straightforward comparison of model outputs across sites, especially within a homogeneous region.

Second, to improve confidence in model results, better understanding of the local sediment budget in a given watershed is key (see Chaplin-Kramer et al., 2016). The variability in calibration values (k_b ranging from 1.8 and 3.5, see Supplementary Material), as well as the large differences between calibrated and uncalibrated values suggest that the model calibration may overcompensate for errors in sediment sources. Better understanding of the sediment budget will improve model interpretation, especially when used to predict environmental changes, i.e. outside model calibration conditions. Unfortunately, relationships between watershed variables and model outputs (including calibrated k_b values) were relatively weak (and with a small sample size), meaning that further work is needed to “regionalize” the calibration process (e.g. determining regional values for k_b). However, we suggest that erosivity is a good proxy for the sediment delivery and propose a relationship (eq. 7) that can be tested in future studies. Alternatively, one practical option to calibrate the model in the absence of observed data is based on the watershed-scale sediment delivery ratio: by using regional relationships between area and this ratio such as those shown in de Vente (2007), it is possible to estimate the average proportion of soil loss that will be transported to the stream for a given watershed.

Third, the model outputs showed substantial sensitivity to DEM resolution. Our analyses suggest that sediment export may be less sensitive to DEM resolution with a simple topography such as the U-shape used in the numerical study. This is because the SDR factor and soil loss (determined by the USLE) may show opposite trends with DEM resolution, compensating their respective effects on sediment export. Practically, if changes in resolutions are anticipated in the analyses, coarser resolutions will show less sensitivity (right-hand side of the curves in Figure 4). More generally, the variability in sensitivity found across the six sites suggest that site-specific analyses may be needed to understand the effect of DEM resolution on particular results (e.g. land use change). Lowering the barriers to conducting sensitivity analyses, similar to those presented in this work, may be a useful practical step to address this type of uncertainty in modeling studies.

Acknowledgements

We thank the Natural Capital Project for their financial support and the useful feedback from our colleagues.

References

Baartman, J.E.M., Masselink, R., Keesstra, S.D., Temme, A.J.A.M., Physics, S., Group, L.M., Geography, S., Group, L., 2013. Linking landscape morphological complexity and sediment connectivity 1471, 1457–1471.

Borselli, L., Cassi, P., Torri, D., 2008. Prolegomena to sediment and flow connectivity in the landscape: A GIS and field numerical assessment. Catena 75, 268–277.

Bracken, L.J., Turnbull, L., Wainwright, J., Bogaart, P., 2015. Sediment connectivity: a framework for understanding sediment transfer at multiple scales. Earth Surf. Process.

Landforms 40, 177–188.

Bracken, L.J., Wainwright, J., Ali, G.A., Tetzlaff, D., Smith, M.W., Reaney, S.M., Roy, A.G., 2013. Concepts of hydrological connectivity: Research approaches, Pathways and future agendas. Earth-Science Rev. 119, 17–34.

Broeckx, J., Vanmaercke, M., Dan, B., Chende, V., Sima, M., Enciu, P., Poesen, J., 2016. Geomorphology Linking landslide susceptibility to sediment yield at regional scale : application to Romania. Geomorphology 268, 222–232.

Catari, G., 2010. Assessment of uncertainties of soil erosion and sediment yield estimates at two spatial scales in the Upper Llobregat basin, (SE Pyrenees, Spain). PhD Thesis. Universitat Autonoma de Barcelona.

Catari, G., Gallart, F., 2010. Rainfall erosivity in the Upper Lobregat basin, SE Pyrenees. Pirineos 165, 55–67.

Cavalli, M., Trevisani, S., Comiti, F., Marchi, L., 2013. Geomorphometric assessment of spatial sediment connectivity in small Alpine catchments. Geomorphology 188, 31–41.

Chaplin-Kramer, B., Hamel, P., Sharp, R., Kowal, V., Wolny, S., Sim, S., Mueller, C., 2016. Landscape configuration is the primary driver of impacts on water quality associated with agricultural expansion. Environ. Res. Lett. 11.

Cheng, C.L., 2007. Evaluating the performance of AnnAGNPS and N-SPECT for tropical conditions. MSc Thesis. University of Hawaii at Manoa, HI.

Conte, M.N., Daily, G.C., Dennedy-Frank, P.J., Eichelberger, B.A., Ghile, Y.B., Kaiser, G.M., Ma, S., McNally, B.W., Rauer, E.M., Ruckelshaus, M.H., Ziv, G., Duggan, J.M., 2015. Enlisting Ecosystem Services: Quantification and Valuation of Ecosystem Services to Inform Base Management. ESTCP Project RC-201113.

Cruise, J.F., Miller, R.L., 1994. Hydrologic modeling of land processes in Puerto Rico using remotely sensed data. J. Am. Water Resour. Assoc. 30, 419–428.

de Vente, J., Poesen, J., Arabkhedri, M., Verstraeten, G., 2007. The sediment delivery problem revisited. Prog. Phys. Geogr. 31, 155–178.

de Vente, J., Poesen, J., Verstraeten, G., Govers, G., Vanmaercke, M., Van Rompaey, A., …, Boix-Fayos, C., 2013. Predicting soil erosion and sediment yield at regional scales: Where do we stand? Earth-Science Rev. 127, 16–29.

Desmet, P.J.J., Govers, G., 1996. A GIS procedure for automatically calculating the USLE LS factor on topographically complex landscape units. J. Soil Water Conserv. 51, 427–433.

Donigian, A.S., Imhoff, J.C., Mishra, A., Deliman, P.N., Regan, E.C., 2009. A Watershed Modeling Framework for Military Installations: A Preliminary Approach and Baseline Model Results, in: Proceedings of the Water Environment Federation, TMDL. pp. 422–440.

Falinski, K.A., 2016. Predicting sediment export into tropical coastal ecosystems to support ridget to reef management. PhD thesis. University of Hawaii at Manoa, Honolulu, HI,.

Goldman-Benner, R.L., Benitez, S., Boucher, T., Calvache, A., Daily, G., Kareiva, P., Kroeger, T., Ramos, A., 2012. Water funds and payments for ecosystem services: practice learns from theory and theory can learn from practice. Oryx 46, 55–63.

Hamel, P., Chaplin-Kramer, R., Sim, S., Mueller, C., 2015. A new approach to modeling the sediment retention service (InVEST 3.0): Case study of the Cape Fear catchment, North Carolina, USA. Sci. Total Environ. 524–525, 166–177.

Hijmans, R.J., Cameron, S.E., Parra, J.L., Jones, P.G., Jarvis, A., 2005. Very high resolution interpolated climate surfaces for global land areas. Int. J. Climatol. 25, 1965–1978.

Hill, B.R., DeCarlo, E.H., Fuller, C.C., Wong, M.F., 1998. Using sediment “fingerprints” to assess sediment-budget errors, North Halawa Valley, Oahu, Hawaii. Earth Surf. Process. Landforms 23, 493–508.

Hoos, A.B., McMahon, G., 2009. Spatial analysis of instream nitrogen loads and factors controlling nitrogen delivery to streams in the southeastern United States using spatially referenced regression on watershed attributes (SPARROW) and regional classification frameworks. Hydrol. Process. 23, 2275–2294.

Hunink, J.E., Droogers, P., 2015. Impact Assessment of Investment Portfolios for Business Case Development of the Nairobi Water Fund in the Upper Tana River, Kenya.

Larsen, M.C., Webb, R.M.T., 2009. Potential Effects of Runoff, Fluvial Sediment, and Nutrient Discharges on the Coral Reefs of Puerto Rico. J. Coast. Res. 25, 189–208.

Leombruni, A., Blois, L., Mancini, M., 2009. First Evaluation of Soil Erosion and Sediment Delivery in the High Part of the Tevere Watershed. EJGE 14.

Lin, S., Jing, C., Coles, N.A., Chaplot, V., Moore, N.J., Wu, J., 2013. Evaluating DEM source and resolution uncertainties in the Soil and Water Assessment Tool. Stoch. Environ. Res. Risk Assess. 27, 209–221.

Liquete, C., Canals, M., Ludwig, W., Arnau, P., 2009. Sediment discharge of the rivers of Catalonia, NE Spain, and the influence of human impacts. J. Hydrol. 366, 76–88.

McDonald, R.I., Shemie, D., 2014. Urban Water Blueprint: Mapping conservation solutions to the global water challenge. The Nature Conservancy: Washington, D.C.

Merritt, W.S., Letcher, R.A., Jakeman, A.J., 2003. A review of erosion and sediment transport models. Environ. Model. Softw. 18, 761–799.

Mondal, A., Khare, D., Kundu, S., Mukherjee, S., Mukhopadhyay, A., Mondal, S., 2016. Uncertainty of soil erosion modelling using open source high resolution and aggregated DEMs. Geosci. Front.

Moore, T.R., 1979. Rainfall Erosivity in East Africa. Geogr. Ann. Ser. A, Phys. Geogr. 61, 147–156.

Mwangi, J.K., Shisanya, C. a., Gathenya, J.M., Namirembe, S., Moriasi, D.N., 2015. A modeling approach to evaluate the impact of conservation practices on water and sediment yield in Sasumua Watershed, Kenya. J. Soil Water Conserv. 70, 75–90.

Phillips, J.D., 1991. Fluvial sediment budgets in the North Carolina Piedmont. Geomorphology 4, 231–241.

Rawls, W., Brakensiek, D., 1989. Unsaturated Flow in Hydrologic Modeling Theory and Practice, in: (Ed.), H.M.-S. (Ed.), Estimation of Soil Wáter Retention and Hydraulic Properties. Fort Collins, U.S.A., pp. 275–300.

Reaney, S.M., Bracken, L.J., Kirkby, M.J., 2014. The importance of surface controls on overland fl ow connectivity in semi-arid environments : results from a numerical experimental approach. Hydrol. Process. 28, 2116–2128.

Renard, K., Foster, G., Weesies, G., McCool, D., Yoder, D., 1997. Predicting Soil Erosion by

Water: A Guide to Conservation Planning with the revised soil loss equation.

Rubel, F., Kottek, M., 2010. Observed and projected climate shifts 1901-2100 depicted by world maps of the Köppen-Geiger climate classification. Meteorol. Z. 19, 135–141.

Sánchez-Canales, M., López-Benito, A., Acuña, V., Ziv, G., Hamel, P., Chaplin-Kramer, R., Elorza, F.J., 2015. Sensitivity analysis of the sediment dynamics in a Mediterranean river basin: global change and management implications. Sci. Total Environ. 502, 602–610.

Sharp et al., 2016. InVEST 3.0 User's Guide. Available at: http://ncp-dev.stanford.edu/~dataportal/invest-releases/documentation/current_release/ [accessed June 2016].

Stock, J.D., Falinski, K.A., Callender, T., 2015. Reconnaissance sediment budget for selected watersheds of West Maui, Hawaii, USA.

Syvitski, J.P.M., Milliman, J.D., 2007. Geology, Geography, and Humans Battle for Dominance over the Delivery of Fluvial Sediment to the Coastal Ocean. J. Geol. 115, 1–19.

Tarboton, D., 1997. A new method for the determination of flow directions and upslop areas in grid digital elevation models. Water Resour. Res. 33, 309–319.

Terrado, M., Acuña, V., Ennaanay, D., Tallis, H., Sabater, S., 2014. Impact of climate extremes on hydrological ecosystem services in a heavily humanized Mediterranean basin. Ecol. Indic. 37, 199–209.

TNC, 2015. Upper Tana-Nairobi Water Fund: A Business Case. Version 2. Nairobi, Kenya.

Verstraeten, G., Poesen, J., de Vente, J., Koninckx, X., 2003. Sediment yield variability in Spain: A quantitative and semiqualitative analysis using reservoir sedimentation rates. Geomorphology 50, 327–348.

Vigiak, O., Beverly, C., Roberts, A., Thayalakumaran, T., Dickson, M., McInnes, J., Borselli, L., 2016. Detecting changes in sediment sources in drought periods: The Latrobe River case study. Environ. Model. Softw. 85, 42–55.

Vigiak, O., Borselli, L., Newham, L.T.H., Mcinnes, J., Roberts, A.M., 2012. Comparison of conceptual landscape metrics to define hillslope-scale sediment delivery ratio. Geomorphology 138, 74–88.

Warne, A.G., Webb, R.M.T., Larsen, M.C., 2005. Water, sediment, and nutrient discharge characteristics of rivers in Puerto Rico, and their potential influence on coral reefs. U.S. Geological Survey Scientific Investigations Report 2005-5206.

White, M., Harmel, D., Yen, H., Arnold, J., Gambone, M., Haney, R., 2015. Development of Sediment and Nutrient Export Coefficients for U.S. Ecoregions. J. Am. Water Resour. Assoc. 51, 758–775.

Wischmeier, W., Smith, D., 1978. Predicting rainfall erosion losses - A guide to conservation planning. U.S. Department of Agriculture. Agriculture Handbook No. 537.

Wu, S., Li, J., Huang, G., 2005. An evaluation of grid size uncertainty in empirical soil loss modeling with digital elevation models. Environ. Model. Assess. 10, 33–42.

Wu, S., Li, J., Huang, G.H., 2008. A study on DEM-derived primary topographic attributes for hydrologic applications: Sensitivity to elevation data resolution. Appl. Geogr. 28, 210–223.

Zhu, S., Tang, G., Xiong, L., Zhang, G., 2014. Uncertainty of slope length derived from digital elevation models of the Loess Plateau, China. J. Mt. Sci. 11, 1169–1181.

Figure 1. The six sites used in this study. The background shows the Köppen-Geiger world main climate zones. (Source: (Rubel and Kottek, 2010)*)*

Figure 2. Synthetic watershed template used for the numerical analyses. Left: DEM and stream network (for the 90m DEM). Right: land two-class LULC raster used for the sensitivity analyses. Right: The C factor of the LULC equals 0.1 in the upper watershed, 0.5 in the bottom part.

Figure 3. Comparison of specific sediment yields from the InVEST model. The panels show results before (crossed squares, left panel) and after (plain squares, right panel) calibration, with the two regional models (BQART, pluses, and FSM, crosses). The "best estimate" on the x-axis is either observed data or prediction from an alternative model with higher level of confidence (see Table 1). Each point represents one watershed (note that not all watersheds had valid predictions from regional models). Note the log-scale.

Figure 4. Trend in sediment export predicted for four DEM resolutions for selected subwatersheds. Some sites show a uniform trend, with sediment export either increasing or decreasing with coarser resolution, while others show non-uniform variations.

Figure 5. Difference in SDR 10th, 50th, and 90th percentiles, sediment export (sed_exp) and total erosion (usle), relative to the 5m resolution. Results are presented for the synthetic watershed with 5% average slope.

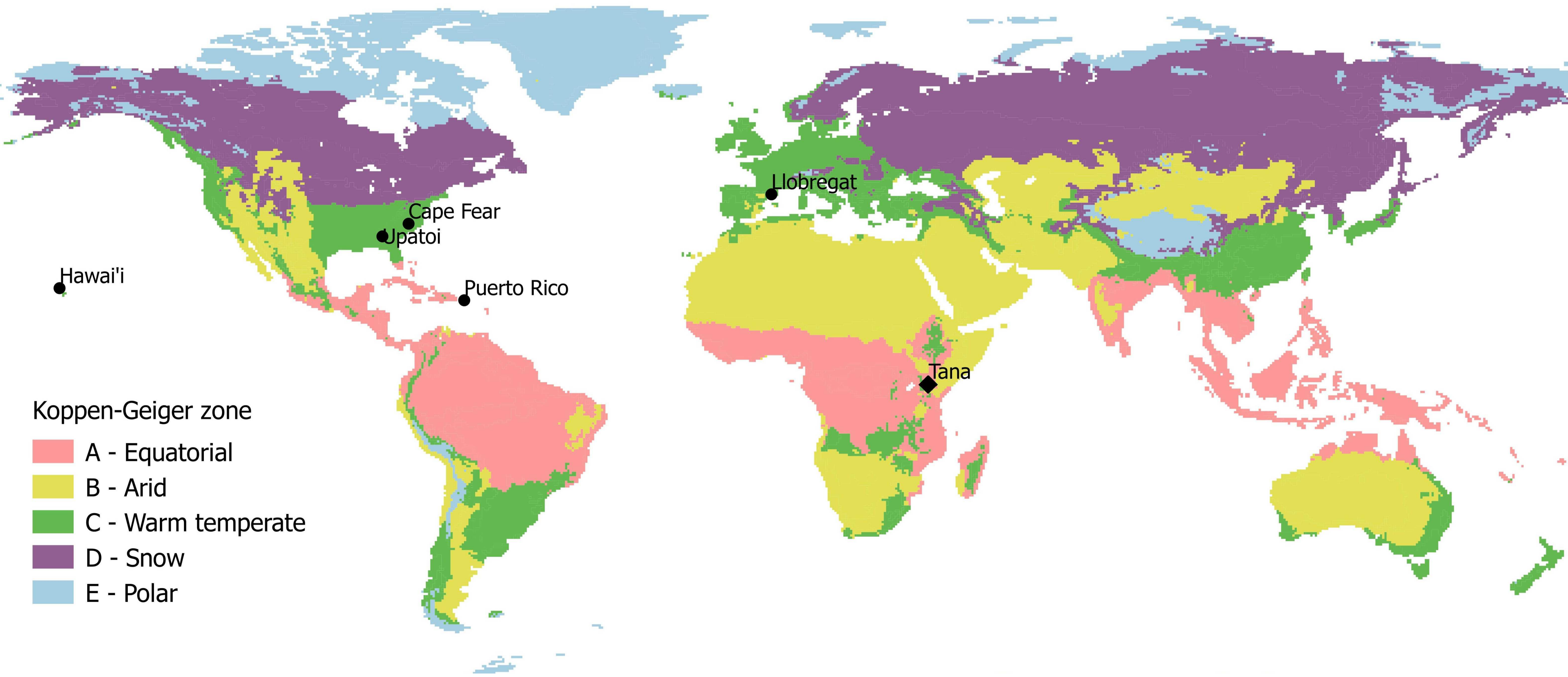
Hawai'i
Cape Fear
Upatoi
Puerto Rico
Llobregat
Tana
Koppen-Geiger zone
A - Equatorial
B - Arid
C - Warm temperate
D - Snow
E - Polar

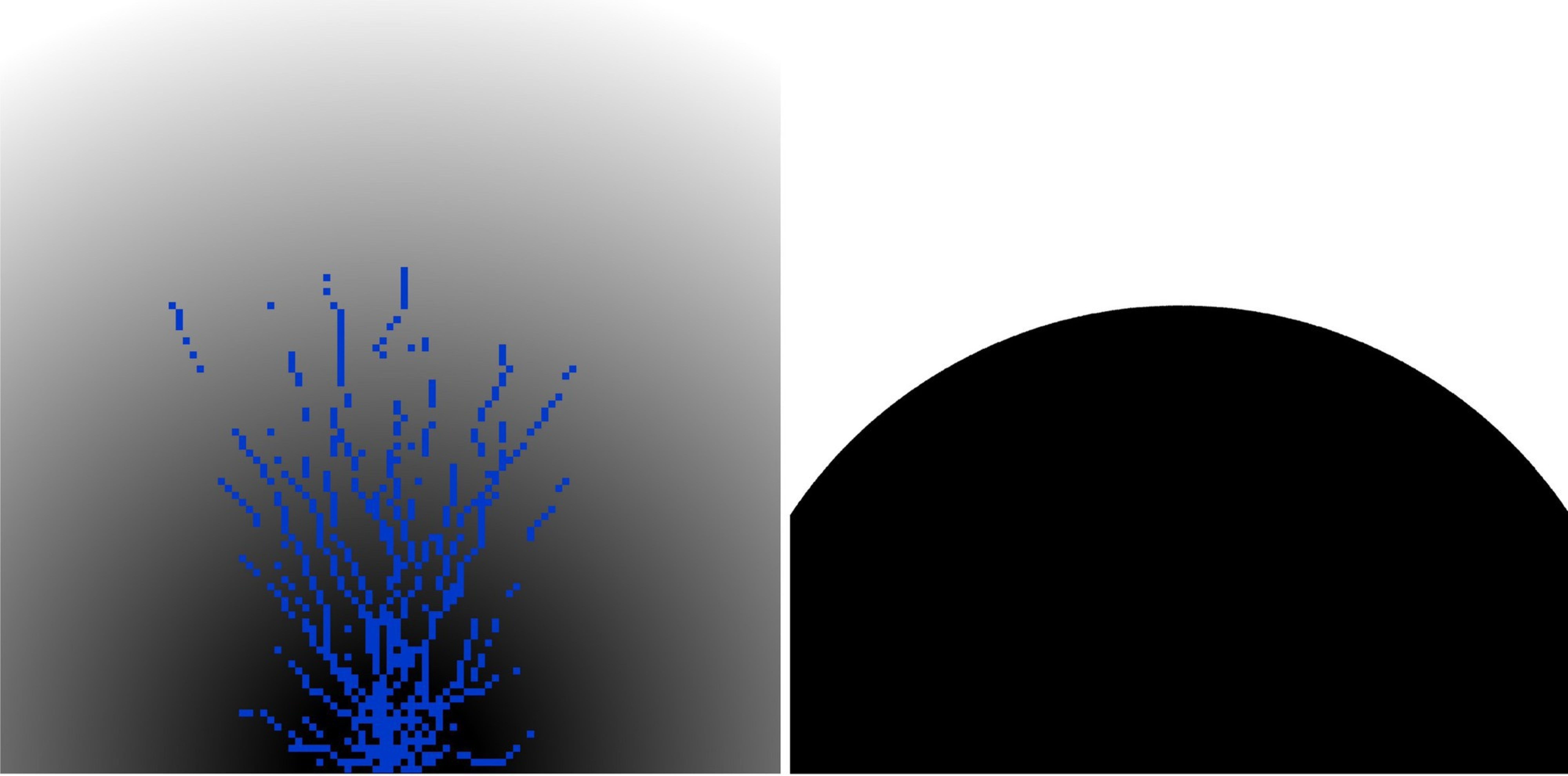

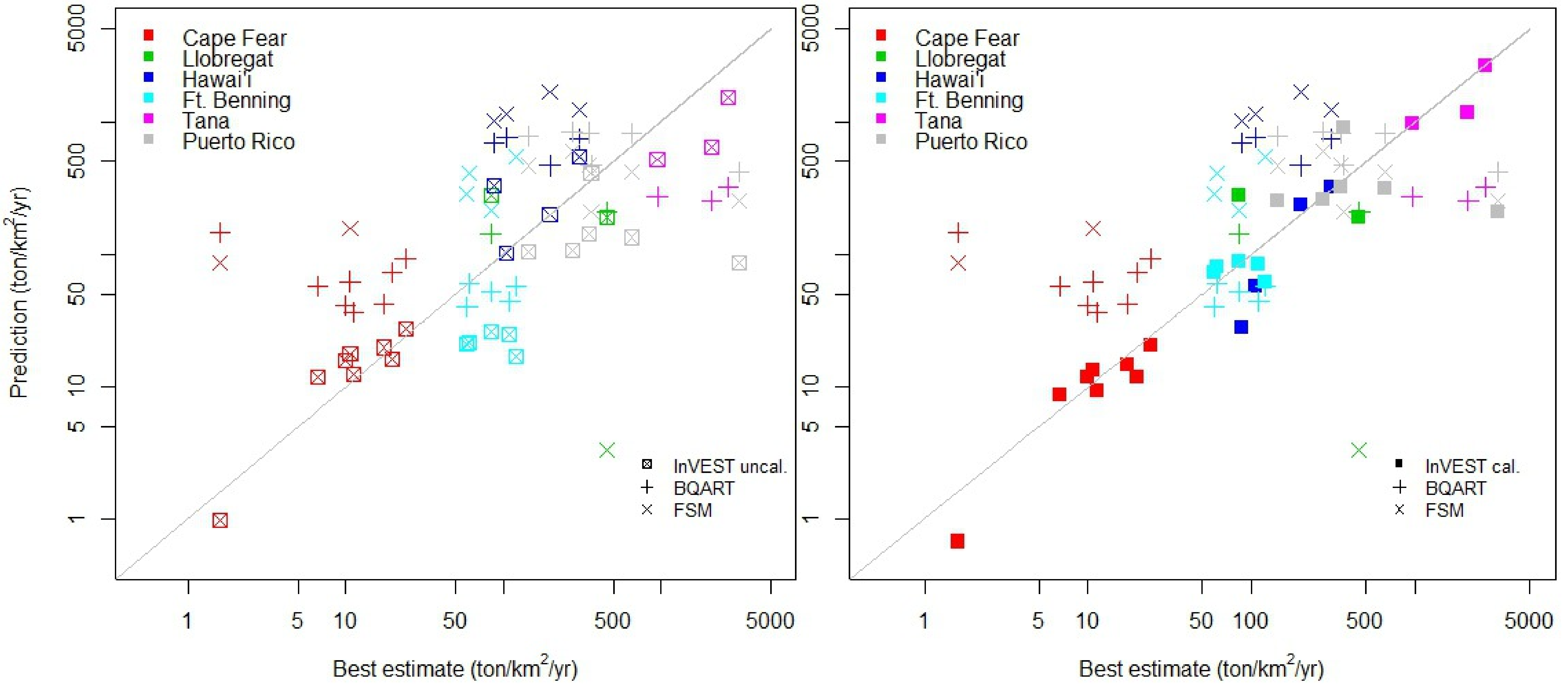
Cape Fear
Llobregat
Hawai'i
Ft. Benning
Tana
Puerto Rico
InVEST uncal.
BQART
FSM
InVEST cal.
Prediction (ton/km²/yr)
Best estimate (ton/km²/yr)
1
5
10
50
100
500
5000

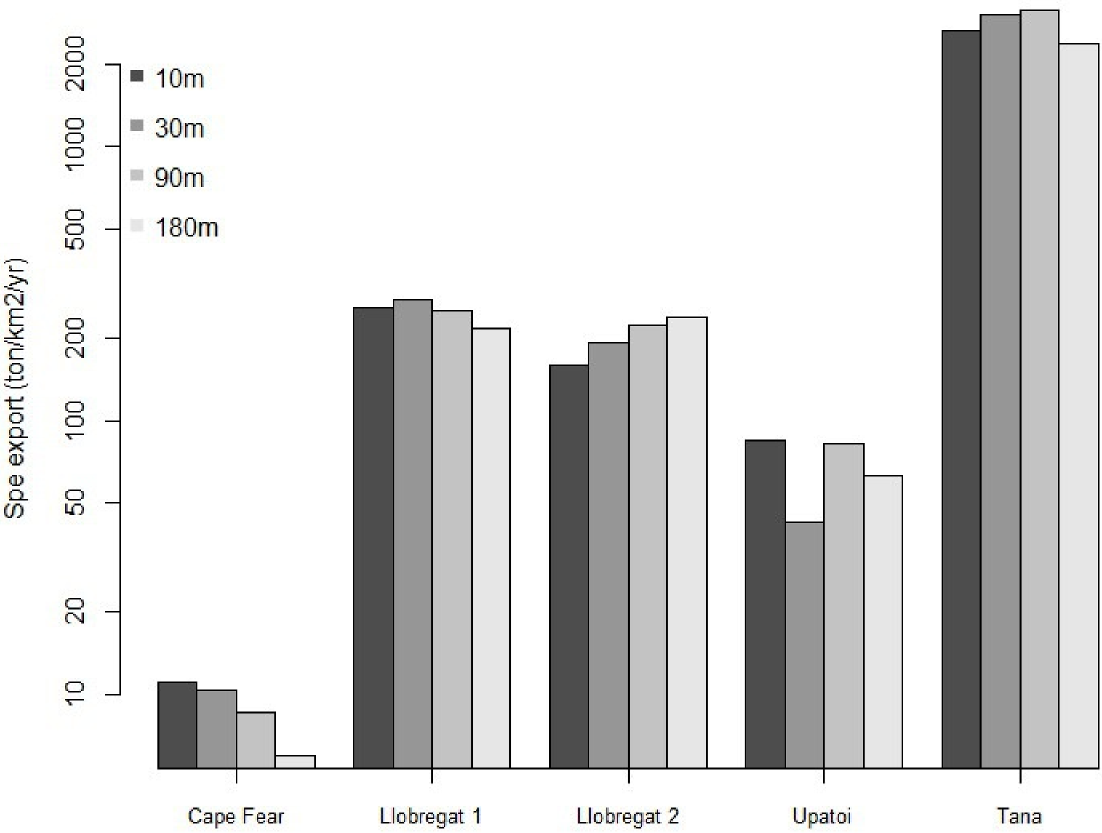

10m
30m
90m
180m
Spe export (ton/km2/yr)
2000
1000
500
200
100
50
20
10
Cape Fear
Llobregat 1
Llobregat 2
Upatoi
Tana

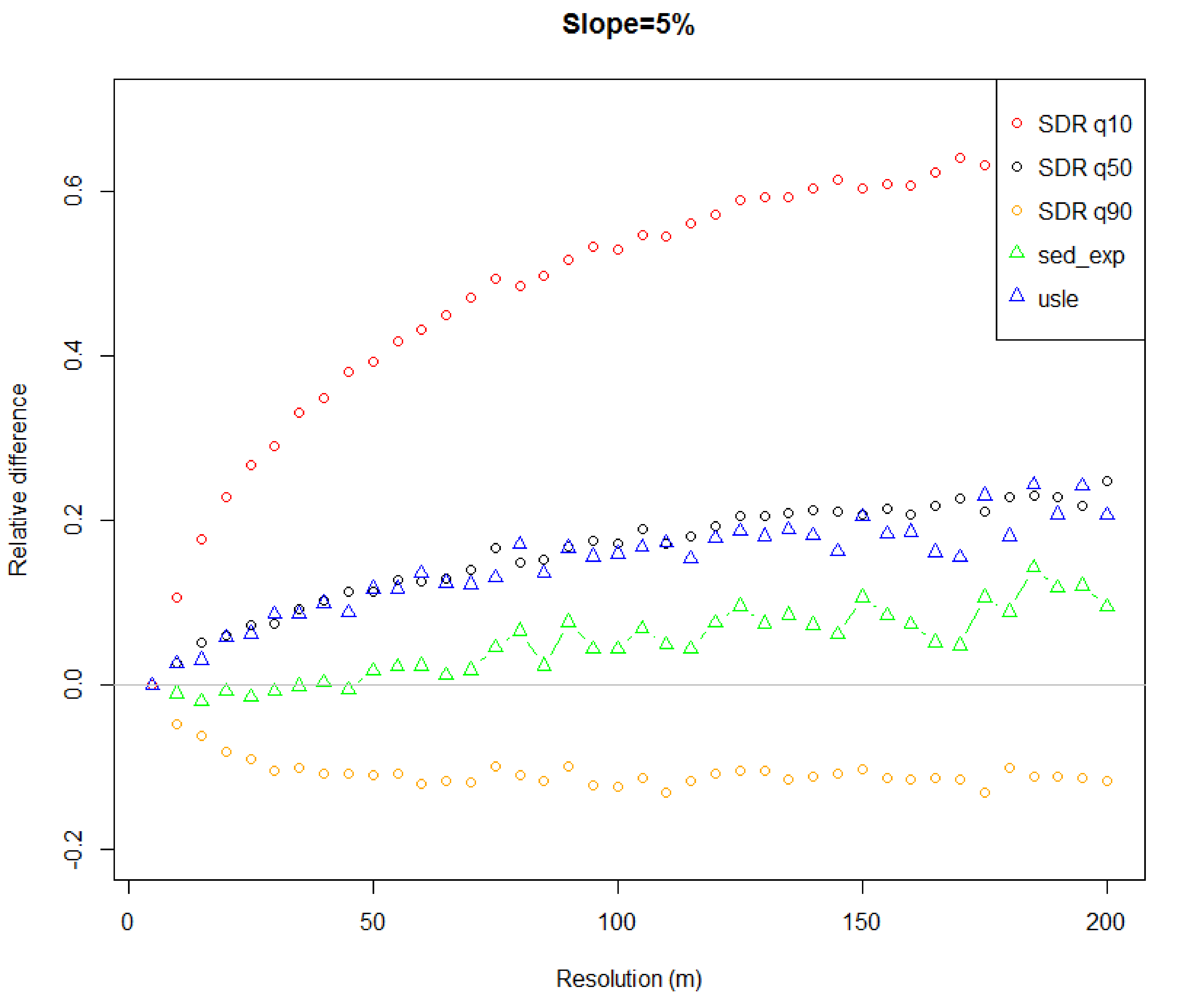
Slope=5%
SDR q10
SDR q50
SDR q90
sed_exp
usle
Relative difference
Resolution (m)
-0.2
0.0
0.2
0.4
0.6
0
50
100
150
200

Table 1. Characteristics of the sites used for the empirical analyses, including watershed properties and InVEST calibration values (IC_0 was kept constant, except for Hawai'i, see Supplementary Material)

	Hawai'i (U.S.)	**Puerto Rico**	**Upatoi (U.S.)**	**Cape Fear (U.S.)**	**Llobregat (Spain)**	**Tana (Kenya)**
Climate	Tropical rainforest	Tropical rainforest	Humid subtropical	Humid subtropical	Hot summer Mediterranean	Tropical wet and dry
Mean annual precipitation (mm)	2500-5900*	1480	1310	1120	600-1000*	1300
Areas (km^2)	[6-10]	[36-123]	[38-886]	[197-13,500]	[500-4900]	[464-2050]
Slope (10-90th) (%)	[17;103]	[8; 42]	[1;10]	[1;11]	[12;62]	[2;20]
Major LULC	Forest (85%) Urban (15%)	Forest (63%) Urban (29%)	Forest (67%) Grassland (19%)	Forest (52%) Urban (17%)	Forest (31%) Grassland (26%)	Crop (84%) Forest (12%)
No. of watersheds	4	6	5	8	2	3
Best estimate	Observed daily load	Observed daily load	SWAT predictions (calibrated on one watershed)	Observed daily load	Regional estimate**	SWAT predictions (calibrated on one watershed)
InVEST calibration (k_b value)	2 (IC_0=0.1)	3.5	3.4	1.8	2	3

* Ranges are given when there is high variability between subwatersheds for a given site (see Supplementary Material)

** based on sedimentation and monthly load data

Table 2. Summary of variables and their statistics analyzed in this study. InVEST metrics are derived from the calibrated model. USLE: Soil loss; IC: Index of connectivity; SDR: Sediment Deliverly ratio; LS: slope-length

	Variable	**Type**	**Statistic**
InVEST metrics			
	Sediment export (ton/yr)	Decimal value	-
	IC (-)	Raster	Median, 10th and 90th
	SDR (-)	Raster	Median, 10th and 90th
	LS	Raster	Median, 10th and 90th
Watershed characteristics			
	Area (km^2)	Decimal	-
	Elevation (m)	Raster	Relief (Min-max)
	Slope (m/m)	Raster	Median, 10th and 90th
	R factor (SI unit)	Raster	Median
	K factor (SI unit)	Raster	Median
	%Forest, Grassland, Urban, Other	Decimal	

*Table 3. Significant correlations between SDR and IC median values, and watershed characteristics. n.s means non-significant at the 0.01-level. *Sed. Export is the calibrated sediment export in ton/km2/yr*

	Sed. Export*	SDR median	SDR 10th	SDR 90th	IC median	LS 90th	tfa	area (km^2)	Relief (m)	Slope median	R median	K median	%Mixed Forest	%Urban	%Croplands	%Other
Sed. Export*	1	0.53	0.44	0.64	0.66	n.s.	0.54	n.s.	0.71	n.s.	n.s.	n.s.	-0.58	n.s.	0.82	n.s.
SDR median	0.53	1	n.s.	0.98	0.9	n.s.	n.s.	-0.53	n.s.	n.s.	0.79	-0.64	n.s.	-0.55	n.s.	-0.66
SDR 10th	0.44	n.s.	1	0.44	n.s.	-0.69	n.s.	n.s.	n.s.	-0.41	n.s.	n.s.	n.s.	-0.49	0.54	n.s.
SDR 90th	0.64	0.98	0.44	1	0.93	n.s.	n.s.	-0.46	n.s.	n.s.	0.69	-0.59	n.s.	-0.57	n.s.	-0.65
IC median	0.66	0.9	n.s.	0.93	1	n.s.	0.62	n.s.	0.54	0.44	0.64	-0.61	n.s.	-0.52	n.s.	-0.59
LS 90th	n.s.	n.s.	-0.69	n.s.	n.s.	1	n.s.	n.s.	0.58	0.77	n.s.	n.s.	n.s.	n.s.	n.s.	n.s.
tfa	0.54	n.s.	n.s.	n.s.	0.62	n.s.	1	n.s.	0.9	n.s.	n.s.	-0.5	-0.66	n.s.	0.64	n.s.
area (km2)	n.s.	-0.53	n.s.	-0.46	n.s.	n.s.	n.s.	1	n.s.	n.s.	-0.56	n.s.	n.s.	n.s.	n.s.	n.s.
Relief (m)	0.71	n.s.	n.s.	n.s.	0.54	0.58	0.9	n.s.	1	n.s.	n.s.	-0.39	-0.58	n.s.	0.8	n.s.
Slope median	n.s.	n.s.	-0.41	n.s.	0.44	0.77	n.s.	n.s.	n.s.	1	0.5	n.s.	0.47	n.s.	n.s.	n.s.
R median	n.s.	0.79	n.s.	0.69	0.64	n.s.	n.s.	-0.56	n.s.	0.5	1	-0.48	0.6	n.s.	-0.4	-0.6
K median	n.s.	-0.64	n.s.	-0.59	-0.61	n.s.	-0.5	n.s.	-0.39	n.s.	-0.48	1	n.s.	n.s.	n.s.	n.s.
%Mix. Forest	-0.58	n.s.	n.s.	n.s.	n.s.	n.s.	-0.66	n.s.	-0.58	0.47	0.6	n.s.	1	n.s.	-0.73	n.s.
%Urban	n.s.	-0.55	-0.49	-0.57	-0.52	n.s.	n.s.	n.s.	n.s.	n.s.	n.s.	n.s.	n.s.	1	n.s.	n.s.
%Croplands	0.82	n.s.	0.54	n.s.	n.s.	n.s.	0.64	n.s.	0.8	n.s.	-0.4	n.s.	-0.73	n.s.	1	n.s.
%Other	n.s.	-0.66	n.s.	-0.65	-0.59	n.s.	n.s.	n.s.	n.s.	n.s.	-0.6	n.s.	n.s.	n.s.	n.s.	1

InVEST

integrated valuation of environmental services and tradeoffs

Sediment delivery model

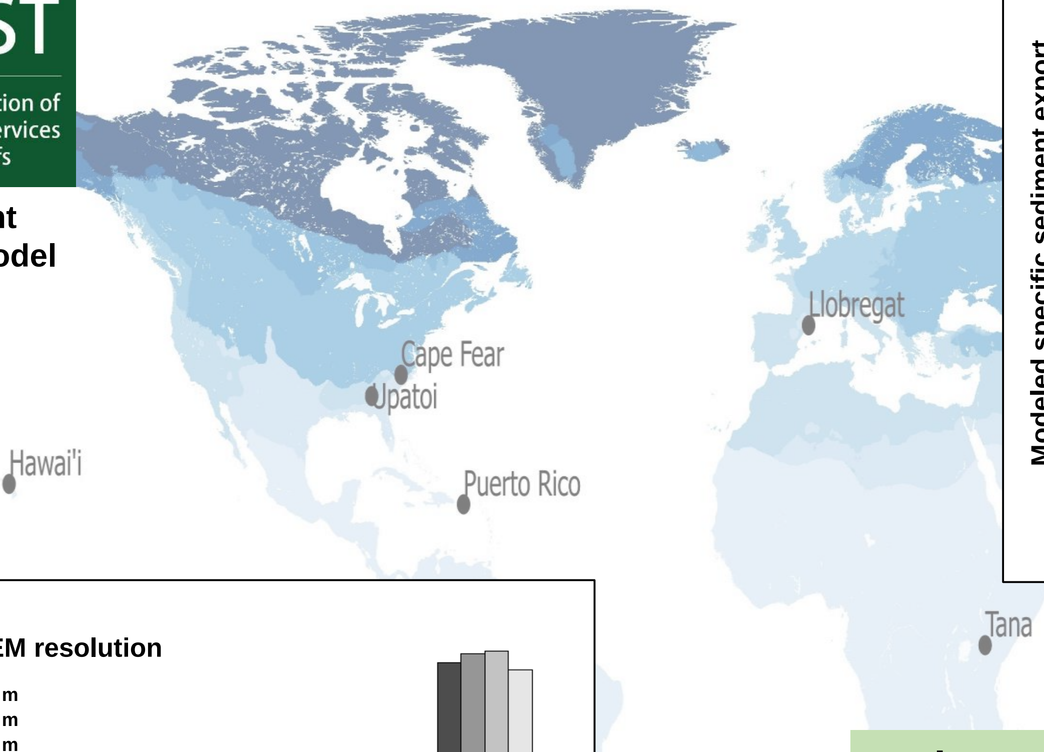

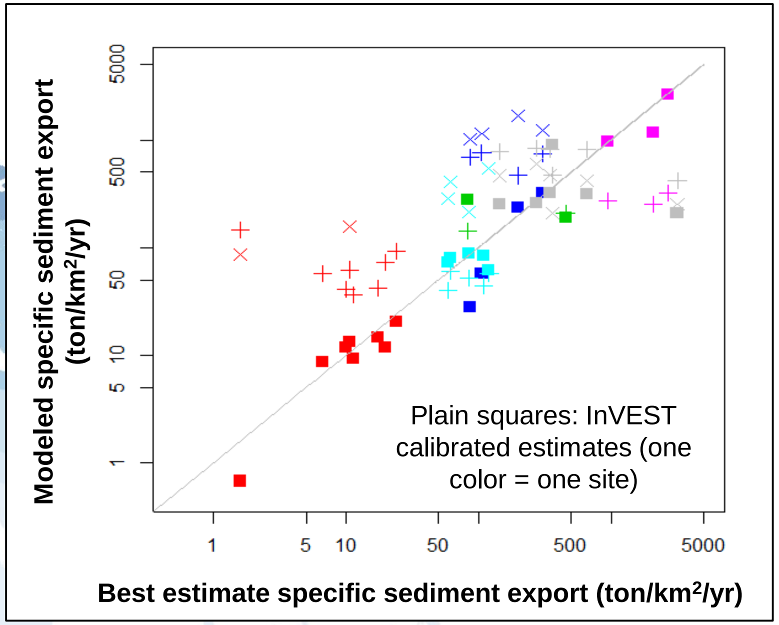

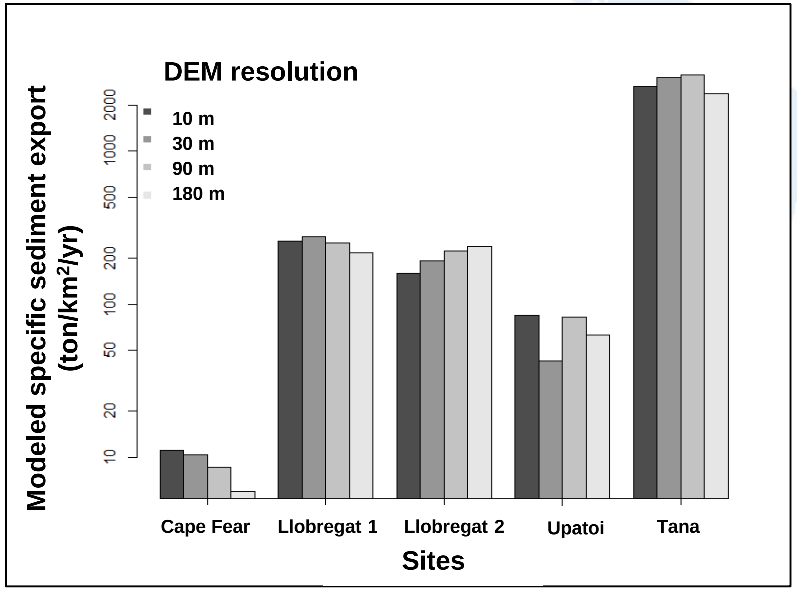

Aim: Modeling uncertainty of geospatial sediment models in six sites with distinct environmental conditions

Results:

The calibrated InVEST model explains variance in sediment export (above)

The model is sensitive to DEM resolution, with the direction and magnitude varying across sites (left)